INVESTIGATION OF THE RELATIONSHIP BETWEEN MICROSTRUCTURE AND APPEARANCE PROPERTIES OF COATING MATERIALS

by

Li-Piin Sung, Maria E. Nadal,
Mary E. McKnight and Jennifer V. Nguyen
National Institute of Standards and Technology
Gaithersburg, MD 20899 USA
and
Chang-Jian Lin
College of Chemistry and Chemical Engineer
Xiamen University
Xiamen, Fujian 361005, China

Reprinted from the 78th Annual Meeting Technical Program of the Federation of Societies for Coatings Technology, October 18-20, 2000, Chicago, IL. Proceedings. A. G. Gilicinski, Editor. Federation of Societies for Coatings Technology, Blue Bell, PA., 534 p., 2000.

NIST
National Institute of Standards and Technology
Technology Administration, U.S. Department of Commerce

Reference: Li-Piin Sung, Maria E. Nadal, Mary E. McKnight, Jennifer V. Nguyen, Chang-Jian Lin, "Investigation Of The Relationship Between Microstructure And Appearance Properties Of Coating Materials," in Proceedings of ICE 2000," A.G. Gilicinski, editor, FSCT, Blue Bell, PA 19422-2350, 2001.

INVESTIGATION OF THE RELATIONSHIP BETWEEN MICROSTRUCTURE AND APPEARANCE PROPERTIES OF COATING MATERIALS

Li-Piin Sung, Maria E. Nadal, Mary E. McKnight, Jennifer V. Nguyen
National Institute of Standards and Technology, Gaithersburg, MD
and
Chang-Jian Lin,
Xiamen Univ., Fujian, China

Abstract

A series of experiments was carried out to investigate the relationship between the microstructure and the appearance of coated materials using confocal laser microscopy and optical scattering metrology. Microstructural properties such as surfaces roughness, pigment particle size and size distribution affect the optical scattering distribution of the sample, resulting in different appearances. In this presentation, preliminary research results on two pigmented coating systems – TiO_2 and metallic-flake pigmented coatings – are presented. By integrating measurements and modeling, a methodology for predicting the appearance of a coating from its microstructure and constituents is proposed.

Introduction

The appearance of a coated object greatly influences a customer's judgment of the quality and desirability of a product. Accurate measurements and rendering of the appearance of an object is in the forefront of technological needs since the advent of industries' use of electronic commerce to market their products. In order to accurately render appearance, one must understand the underlying physics of appearance. The appearance of a coated object (e.g. color, gloss) is a complex function of the light incident on the object, the optical scattering characteristics of the material, and human perception. The optical scattering properties of a material depend on its surface topography and subsurface microstructure. Thus, the first step for accurately predicting and rendering the appearance of objects is to gain a better understanding of the microstructural and scattering properties of the object under investigation.

To identify the key parameters in microstructure characterization and to predict the scattering properties using microstructure data, the Measurement Science for Optical Reflectance and Scattering project team at the National Institute of Standards and Technology (NIST) has been conducting a series of studies on coated materials having different microstructural properties (e.g. surface roughness, pigment size, and pigment spatial distribution). Two model systems – a clear coating on a

black substrate and coatings containing pigments – were selected. A recently completed study of a clear coating model system demonstrated good agreement between measured and modeled reflectance.[1] Using the same methodology, we are studying pigmented coatings. A series of samples varying in their microstructural properties (pigment materials, sizes, dispersion, and spatial distribution) were used to investigate the relationship between the nature of the microstructure and the optical reflectance properties of the coatings. In this paper, we will present preliminary results on microstructure and optical properties of two pigmented coatings – TiO_2 and metallic flakes – using laser scanning confocal microscopy (LSCM) and optical scattering. A general approach for developing and integrating measurement and modeling efforts will also be discussed.

Experimental

Samples

Two representative pigmented coatings – TiO_2 and metallic flakes – were used in this study. TiO_2 pigmented coatings were prepared at NIST. TiO_2 pigments (obtained from Millennium Inorganic Chemical Co.[a]) were well dispersed into an acrylic-urethane binder, and were coated on release paper or glass substrates using a drawdown-blade or spin-casting techniques. Three gray, aluminum (Al)-flake pigmented samples provided by DuPont[a] were chosen. These samples have the same pigment volume concentration (PVC) but different pigment sizes. The sample designated "C" contains relatively coarse Al flakes (20 μm to 30 μm in diameter). For sample "F", the Al flakes were relatively fine (1 μm to 10 μm) and sample "C-F" contain an equal mixture of coarse and fine Al flakes.

Instrumentation

A Zeiss model LSM510[a] laser scanning confocal microscope (LSCM) was employed to characterize the microstructure of the coatings. LSCM utilizes coherent light and collects light exclusively from a single plane (a pinhole sits conjugated to the focal plane) and rejects light out of the focal plane. The wavelength of the laser (543 nm or 488 nm), numerical aperture of the objective, and the size of the pinhole dictate the resolution in the thickness or axial direction.[2] By moving the focal plane, single images (optical slices) can be combined to build up a three dimensional stack of images that can be digitally processed. In this paper, LSCM images in intensity or depth profile presentations are projections of overlapping optical slices (a stack of z-scan images) with each z-step ranging from 0.3 μm to 1.5 μm depending on the pigment size and distribution.

In-plane bidirectional reflectance distribution function (BRDF) measurements of the coatings were performed using the NIST spectral tri-function automated reflectance reflectometer (STARR).[3] The three functional operations of the STARR facility are absolute measurements of bidirectional, specular, and directional – hemispherical reflectance over the wavelength range of 200 nm to 2500 nm. The incident radiant flux is a monochromatic, collimated, polarized beam with a diameter of 14 mm and a bandwidth of 10 nm. For bidirectional measurements, a lens focuses either the collimated incident beam or the image of the front of the sample onto a silicon photodiode. The sample is

[a] Certain instruments or materials are identified in this paper in order to adequately specify experimental details. In no case does it imply endorsement by NIST or imply that it is necessarily the best product for the experimental procedure.

positioned either in or out of the incident beam using two orthogonal translation stages, that determine the incident angle of the beam on the sample and the viewing angle of the photodiode.

Results and Discussion

Image and data processing of LSCM results from two pigmented coating systems are compared to optical scattering reflectance measurements.

TiO_2 Pigmented Coatings

Figures 1a-c show LSCM images of the TiO_2 pigments in an acrylic-urethane binder for three pigment volume concentrations (PVC). It is clear that the LSCM technique is a powerful visual aid for charactering the pigment size (or cluster) size and dispersion as a function of the pigment volume concentration. The depth and transverse resolutions for LSCM images in Figure 1 were estimated around 256 nm (depth) and 210 nm (transverse) respectively for an objective having a numerical aperture = 1.3 and incident laser wavelength = 488 nm.[2] Scanning electron microscopy (SEM) measurements were also carried out on the 5 % PVC samples to determine the pigment particle size and spatial distribution in both flat and fracture surfaces.[4] It was confirmed that the average single TiO_2 pigment size was around 300 nm, which was consistent with data provided by the manufacturer. The comparison between SEM and LSCM images indicated that LSCM can provide consistent and adequate results for a non-destructive, fast measurement.

The point-point (pair) autocorrelation in real space[5] was calculated for the three TiO_2 samples by digitizing a two-dimensional (2D) image, which consists of a single optical slice, and is presented in Figure 1d. The autocorrelation of the LSCM measurements on the sample containing NIST standard reference materials (SRM) 1690 (900 nm) polystyrene latex (PSL) spheres using the same technique was also included for comparison. Using the autocorrelation function, a 3D image can be reconstructed with important parameters such as the pigment or cluster size and location in 3D for modeling for scattering theory. The cluster size (in diameter) obtained from Figure 1d assuming a spherical cluster in the 3D for the three samples were estimated to be about 390 nm (1.5 % PVC), 240 nm (2.5 % PVC), and 228 nm (5 % PVC). The estimated expanded uncertainty (k=2) is about 50 nm. This indicated that the average size of a cluster in the 1.5 % PVC coating was slightly larger that of a single TiO_2 particle, and the average size of the clusters was reduced to the diameter of a single TiO_2 particle in the 2.5 % and 5 % PVC coatings.

The cluster size and spatial distribution of the pigments can also be obtained from a two-dimensional (2D) Fast Fourier Transformation (FFT) technique.[6] Figure 1e shows the circularly-averaged scattered intensity from the FFT power spectrum as a function of q in a double algorithm plot for the three samples shown in Figures 1a-c. Here q is the frequency, which is inversely proportion to the spatial domain size. In general, the FFT power spectrum is proportional to the scattered intensity and q is related to the scattering angle θ ($q \sim \sin\theta$), as shown in Figure 1f. The q dependence of the scattered intensity for the three samples are similar, indicating that the cluster size and spatial distribution are similar for the three samples. The value of the cross-over q*, which is inversely proportional to the cluster size of the pigment, increases slightly as PVC increases. Scattering measurements, such as small angle neutron and light scattering, will be also carried out and the results will be compared to the FFT analysis of LSCM images.

Al-Flake Pigmented Coatings

The most commonly used metallic pigments in the automobile industry are aluminum (Al) flakes. There are a wide range of flake sizes. The orientation of the flakes in a coating depends on the surface treatments of the flakes and the processing conditions.[7] In this work, we focus on the effect of the flake size on the appearance of an Al-flake pigmented sample. Figure 2 shows the LSCM images of the three gray Al-flake pigmented samples. The first layer of the Al flakes appeared around 60 μm below the air-coating interface and most of the Al flakes were oriented parallel to the surface of the sample. The upper set of images represents the intensity profile and the lower set of images represents the depth profile of the pigment distribution in a series of z-scan optical slices. The dark regions indicate the absence of Al flakes in the probed region. The size of the Al flakes ranged from 1 μm to 30 μm, and the shapes of the flakes varied from platelet-like to particle-like. Variations in size and shape of flakes resulted in different spatial distributions, which caused differences in appearance. For example, sample C (Figure 2a) with coarse flakes exhibited a grainy finish (or "glitter") and sample F with fine flakes (Figure 2c) exhibited a smoother finish with no noticeable glitter.

From the depth-profile, we deduced the near-surface pigment density in the film. For example, the measured maximum depth of sample C was about 27 μm, while the maximum depths for sample C-F and F were 19 μm under the same illumination conditions. This implies that sample C had a lower near–surface density, which may introduce higher diffuse scattering. To verify this assumption, we performed the 2D FFT of the LSCM images. From the 2D FFT, we can extract the orientation and spacing of the structure of the flakes in the original spatial (real space) domain. The circularly averaged scattered intensity from the FFT data of the LSCM images were also compared with BRDF data. Figure 3a shows the circularly-averaged magnitude of the FFT power spectrum as a function of q for the three samples shown in Figure 2. Figure 3b shows BRDF data for the three samples at an incident angle of 45^o and viewing angle of $\pm 10^o$ with respect to the specular angle. The BRDF data were indistinguishable in the specular (near $\theta = 45^o$) region because all of the samples contained a smooth top layer of the same polymer binder, and the angular resolution of the STARR near the specular angles is limited by its aperture. However, sample C had a relatively higher off-specular (diffuse) component than samples C-F and F. This difference in BRDF data was a result of different subsurface microstructure. The FFT data (Figure 3a) exhibited a similar trend as BRDF data in the off-specular region. Contrary to the BRDF data, the FFT data did not include the scattering information from the top layer of clear polymer binder and the scattering depth of the sample (FFT data was obtained using a 2D projected LSCM images). Direct comparisons of the BRDF and FFT data are difficult because the viewing area is different in these two measurements. Thus, factors such as the non-uniformity of the Al-flake distribution as well as artifacts induced through image processing could contribute to the difference in the BRDF and FFT data. Nevertheless, this study implies that LSCM images can be used to predict the trends in scattering properties. This application will be useful for examining and characterizing the determinant microstructure of products under different processing conditions and for predicting the appearance of the final product using reflectance models developed from microstructure data.

In addition to the FFT image analysis method, we are using the same methodology developed for the clear coating system to model a pigmented coating system. Real-space topography data, as shown Figures 4a (sample C) and 4b (sample F), are used for theoretical modeling of scattering using a ray method to calculate the reflectance properties of a coating, which can be compared to the measured BRDF data. Efforts in developing a theoretical modeling for describing the relationship between the microstructure and optical scattering, and rendering the appearance of a coated object using calculated and measured BRDF data are under investigation.

Summary

We have proposed a methodology for predicting the appearance of a coating from its microstructure and constituents. By integrating measurements and modeling, we can relate the optical scattering properties to its microstructures. In the first step, we have demonstrated that laser scanning confocal microscopy is a powerful technique for characterizing coating microstructure. Using FFT image analysis, the microscopic data can be related to the optical scattering measurements. In addition, real-space topography data or 3D reconstruction images can be used for theoretical modeling of scattering to calculate the optical properties, which can be compared to the measured BRDF data.

Acknowledgement

This research is part of the Measurement Science for Optical Reflectance and Scattering project at NIST. For more information, please visit the project web site, http://www.ciks.nist.gov/appmain.htm.

References

(1) McKnight, M.E.; Marx, E.; Nadal, M.E.; Vorburger, T.V.; Barnes, P.Y.; Galler, M.(2000), "Measurements and predictions of light scattering by clear epoxy coatings," to be submitted to Applied Optics.

(2) Corle, T.R.; Kino, G.S. (1996), "Confocal Scanning Optical Microscopy and Related Imaging Systems," *Academic Pres,s*.

(3) Barnes, P.Y; Early, E.A; Parr, A.C.(1998), "Spectral Reflectance," *NIST Special Publication*, 250-*28*.

(4) Sung, L.; Nadal, M.E.; Stutzman, P.; McKnight, M.E. (2000); "Characterization of coating microstructure using laser scanning confocal microscopy," *PMSE Preprint*, in press.

(5) Bentz, D.P. and Martys, N.S.(1994), *Transport in Porous Media*, 17, 221.

(6) Russ, J.C. (1995), "The Image Processing Handbook," 2nd ed. *CRC Press*.

(7) Wicks, Z.W.; Jones, F.N. Jr.; Pappas, S.P. (1992), "Organic Coatings: Science and Technology," *John Wiley & Sons, Inc*.

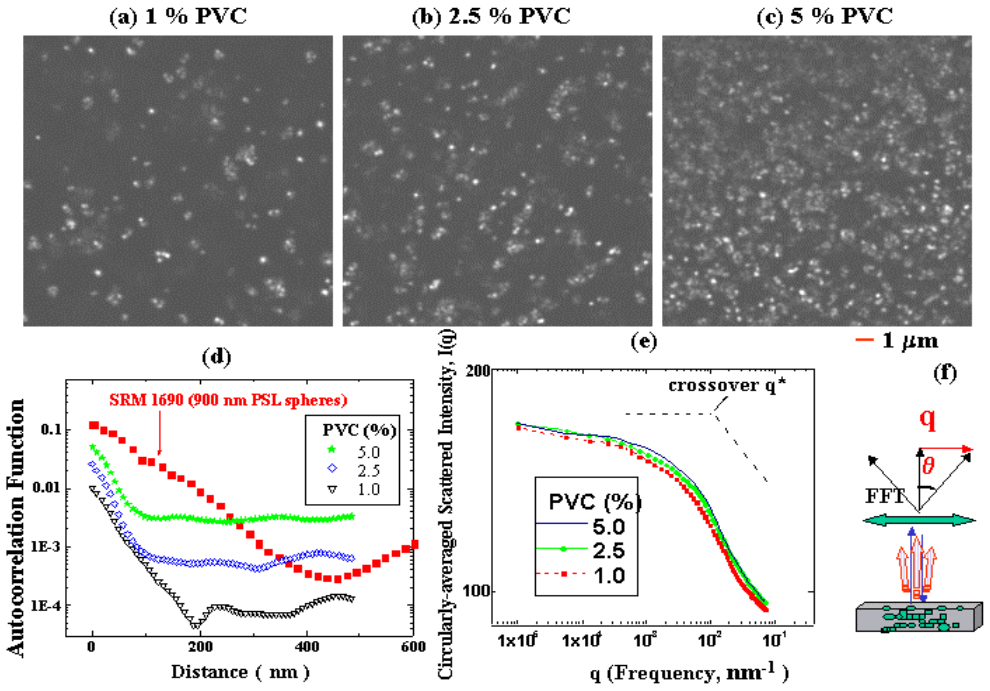

Figure 1. (a)-(c) LSCM images of TiO_2 pigments in an acrylic-urethane binder for three different pigment volume concentrations (PVC). (d) Autocorrelation function. (e) Circularly averaged scattered intensity obtained from Fast Fourier Transformation (FFT) of LSCM images for three different PVC samples. (f) A drawing illustrates the relationship between q and scattering angle.

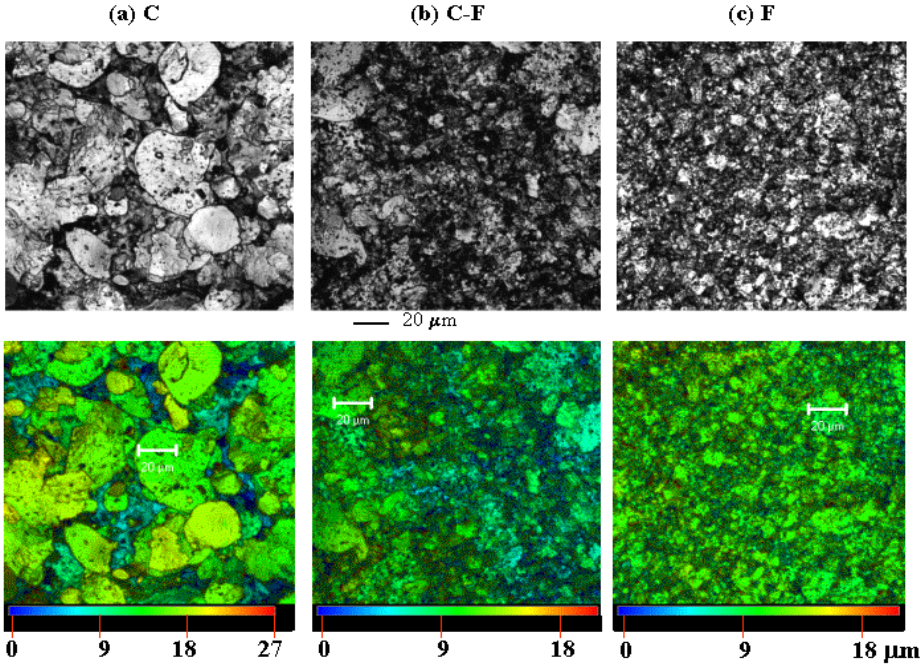

Figure 2. LSCM images of three gray, Al-flake pigmented coatings having the same PVC but containing different pigment sizes, (a) coarse, (b) 50 % coarse with 50% fine, and (c) fine Al flakes. Upper images are intensity presentations, and the bottom images are depth profile projections.

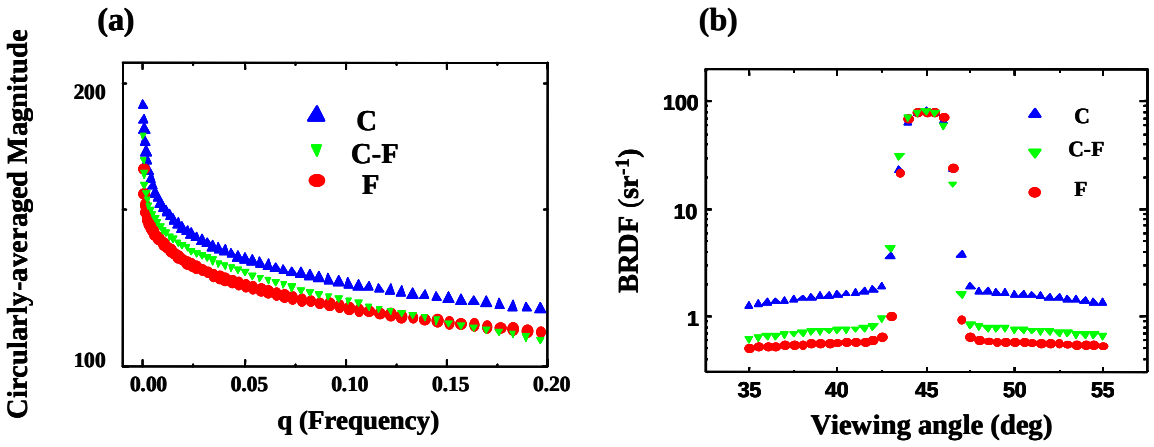

Figure 3. (a) Circularly-averaged magnitude of FFT power spectrum as a function of frequency q. (b) BRDF data of coarse (C), mixture of coarse and fine (C-F), and fine (F) Al-flake pigmented coatings at an incident angle of 45° and viewing angles of ± 10° with respect to the specular geometry. The expanded uncertainties of the BRDF data are less than ± 0.5 % (k=2) and the size of the error bar is smaller than the size of the symbols used in the graphs.

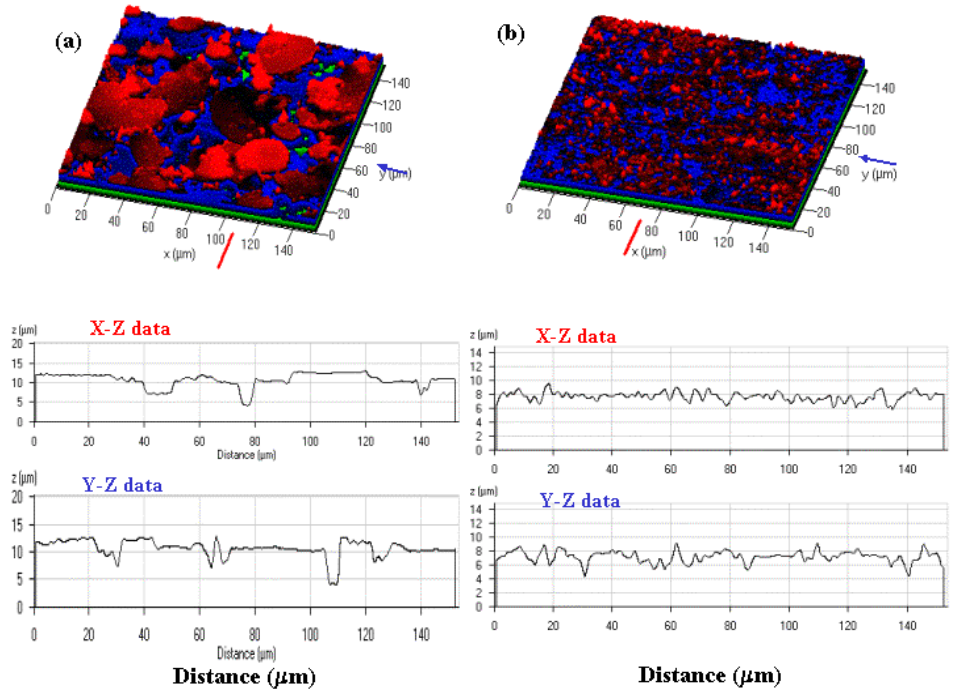

Figure 4. 3D topographic presentations of the same LSCM images for samples C and F shown in Figure 1.